

COMPUTATIONAL INSTABILITY ARISING FROM YIN-YANG BOUNDARY

M. Sakamoto , K. Kawano, K. Aranami, T. Hara, H. Kusabiraki, J. Ishida, C. Muroi

Japan Meteorological Agency, Tokyo, Japan

and

Y. Kitamura

Meteorological Research Institute, Tsukuba, Ibaraki, Japan

1. Introduction

A Yin-Yang grid is a composite mesh proposed by Kageyama and Sato (2004). The technique allows us to create a global numerical weather prediction (NWP) model using a regional dynamical core.

In 2009, Japan Meteorological Agency (JMA) initiated a fundamental research to develop a global non-hydrostatic NWP model, and a Yin-Yang grid model, which is planned to use a regional model ASUCA (Ishida et al. 2010), has been one of candidates for a further development. Generally grid models don't require all-to-all message passing interface (MPI) communication which spectral models require. Therefore when considering an operational use of the high resolution global non-hydrostatic model at a hyper parallel computing environment, grid models like a Yin-Yang grid have an advantage.

There are several ways to compose a Yin-Yang grid (Qaddouri and Lee 2011, Baba et al. 2010, Peng et al. 2006). The selection of the procedures is mainly depending on discretization methods and advection or flux calculation schemes. So far, the finite volume

method (FVM) with the boundary region exchange (BRE) method (Sugimura et al. 2006) is examined in this study.

In the course of developing shallow-water and three-dimensional models, we have encountered computational stability problems. We have analyzed results to overcome the issues, and found that some of the problems are closely related to discretization methods and flux calculation schemes.

2. Non-hydrostatic model ASUCA

ASUCA is a regional NWP model developed by JMA, and will come into operation by the spring of 2014 as a very high resolution (2km grid) operational forecasting system. ASUCA adopts features below;

- The finite volume method (FMV) is used with a flux limiter by Koren (1993), which enables us to keep monotonicity and preserve conservation of scalar predictors without using any artificial numerical diffusion / viscosity to maintain computational stability,
- ASUCA can accommodate some map projections, using the general coordinate transformations, including

Corresponding author address:
Masami Sakamoto,
Numerical Prediction Division, Japan Meteorological Agency,
1-3-4, Otemachi, Chiyoda, Tokyo 100-8122, Japan.
e-mail: masami.sakamoto-a@met.kishou.go.jp

- the Lambert conformal conic projection for the regional (domestic) forecasts
 - the spherical curvilinear coordinates (latitude - longitude projection) which is necessary for Yin-Yang grid expansion.
- ASUCA adopts a 3rd order Runge-Kutta time integration scheme proposed in Wicker and Skamarock (2002).

In this study, a Yin-Yang grid using ASUCA is examined.

The flux limiter by Koren (1993) can appropriately propagate a large (more than 10 grid long) signal with a quick motion (when courant number is close to 1). However it tends to dump a small (less than eight grid) signal with small velocity (courant number less than 0.2) as shown in Fig 1. The flux limiter contributes to the computational stability.

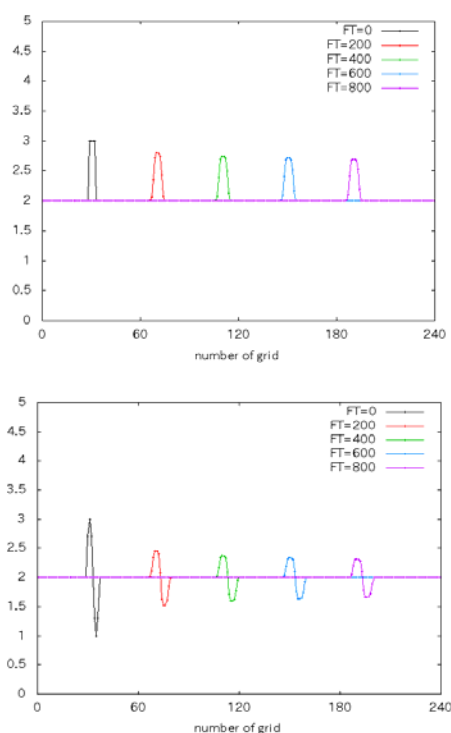


Fig. 1 Advection tests ($\partial h/\partial t = u \nabla h$) by FMV with Koren (1993). The grid interval and time step are unity ($\Delta x=1, \Delta t=1$). [Upper Panel] velocity $c=0.2$ (courant number: 0.2) with $4\Delta x$ long rectangular signal. [Lower] $c=0.2$ and an $8\Delta x$ long sine curve.

3. Problems and Discussions

3.1 Flux Adjustment at the Boundary

There are some techniques to ensure the accuracy of the conservation of scalar predictors by adjusting flux at boundaries. Peng et al. (2006) proposed such a technique named the conservative constraint (CC) for the Yin-Yang boundary. We examined CC for the shallow water test case 2 of Williamson et al. (1992), and obtained the result of a two-day integration shown in the upper panel of Fig. 2. It is quite different from the lower panel of Fig. 2, which is the result from the same test without CC. Calculation halted before 5 day integration for CC due to computational instability. Note that no artificial numerical diffusion / viscosity is used.

We examined a one dimensional shallow - water test, in which two grid systems are joined through exchange of predictors at the boundary (see Fig. 3). Both grid systems have 204 grid (100 x 204 m) long calculation domains, and a cosine bell shaped signal is given as an initial perturbation near the center

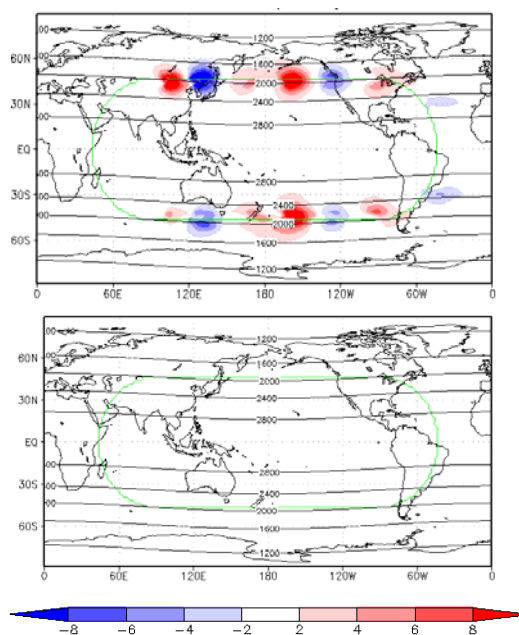


Fig. 2 Thickness (contour) and its error (shade) after 2day forecast with the conservative constraint (upper) and without it (lower). The inclination angle of the flow: $\alpha=0.05$ rad.

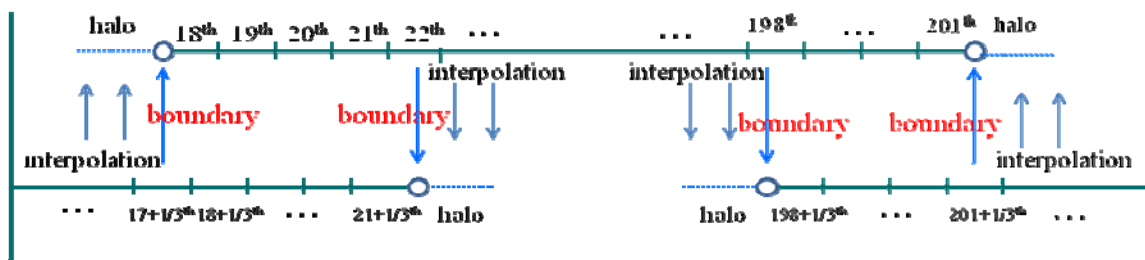


Fig.3 Schematic diagram of a one dimensional shallow water test with the boundary region exchange (BRE) composite mesh. Results with and without boundary momentum exchange are examined. The overlap lengths are $4+1/3$ and $3+2/3$.

of the upper grid system. For this test, momentum exchange at both ends of the calculation domains is equivalent to CC.

The results with (upper) and without (lower) the boundary momentum exchange are shown in Fig.4. Reflection at the left end (boundary) of the upper grid system is seen in one with the boundary momentum exchange. Equations we used here are

$$\frac{\partial \mathbf{h}}{\partial t} = \nabla(\mathbf{u}\mathbf{h}), \quad (1)$$

$$\frac{\partial(\mathbf{u}\mathbf{h})}{\partial t} = \nabla(\mathbf{u}^2\mathbf{h}) + \mathbf{g}\mathbf{h}\frac{\partial \mathbf{h}}{\partial \mathbf{x}}, \quad (2)$$

where h is thickness (m), u is velocity (m/s), g is the acceleration of the gravity (m/s^2), t is time (sec), and $\Delta t = 10$ sec. When the temporal change rate (left side) in (2) is determined by the momentum (uh) at the other grid system rather than the distribution of thickness and momentum in own grid system, the boundary can be a non-holonomic, where reflection can occur. As is seen in case 2 of Williamson et al. (1992), computational instability can arise from the boundary momentum exchange named CC.

3.2 Discrepancy within the overlapped area

As for BRE, both (yin / yang) grid systems forecast independently for the overlapped area only exchanging information along the boundary region (the thick blue and red parts in Fig. 5). Serious problems might happen

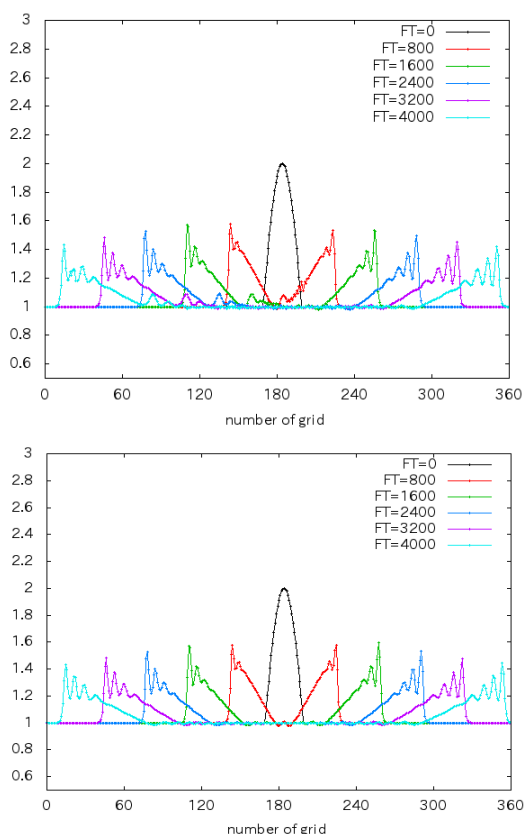


Fig. 4 Forecast results of thickness (m) with the boundary momentum exchange (upper), without it (lower). FT denotes number of time steps integrated.

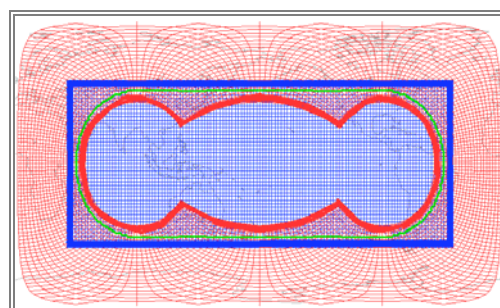


Fig. 5 Schematic diagram of the boundary region exchange (BRE). The blue grid (yin-grid) receives information at the thick blue region, and the red grid (yang-grid) receives at the thick red area. Forecasts for the overlapped area between the thick areas are done independently in both grids.

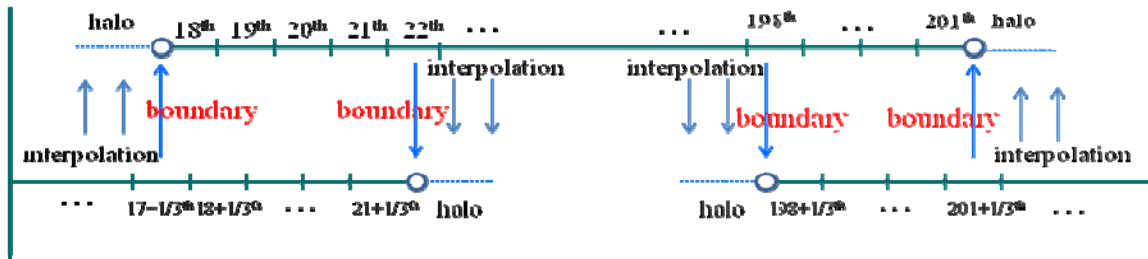


Fig.6 Schematic diagram of a one dimensional shallow water test with two grid long dent in the overlapped area for the upper grid.

when there are apparent discrepancies between the two grid systems within the overlapped area. A one dimensional shallow-water test similar to one in the previous section is examined to find what happens around the boundary in such a condition. The overlapped lengths are $8+1/3$ and $7+2/3$ grids (Fig.6) instead of $4+1/3$ and $3+2/3$ for the previous section (Fig.3). As the initial field, a 2-grid long dent (see Fig.7) is given in the overlapped area only for the upper grid system of Fig. 6.

The results are shown in Fig. 8. Noises derived from the boundary are propagating in both directions, but they are not diminishing. This seems to result from the resonance within the overlap, since the frequency of the noise seems to be quite constant.

We have tried various measures to reduce the noise, and found a filter proposed by Shapiro (1971) is one of the most effective ways to moderate the issue as is shown in

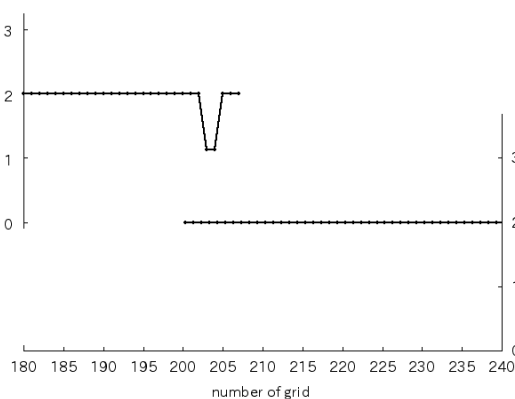


Fig. 7 Initial field of thickness (m) for the experiment with the two grid dent in the overlapped area.

Baba et al. (2010). Shapiro's filter damp only short-waves (less than eight grid signals), and the filter effectively damps noises (Fig.9).

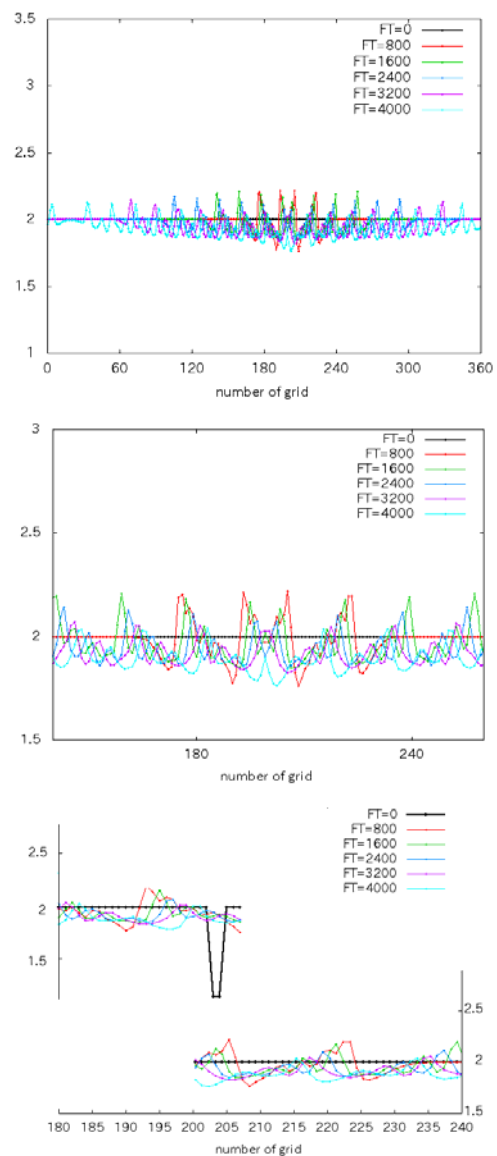


Fig. 8 Thickness referring value from 20 to 199th of the upper grid, from $200+1/3$ to $19+1/3$ th of the lower (Upper and Middle). That for each grid around right boundary (Lower).

4. Summary

Two types of computational instabilities arising from the Yin-Yang boundary are analyzed using one dimensional shallow-water model tests. These are related to

- A) influence by a flux adjustment at the boundary,
- B) discrepancy within the overlapped area.

As for problem A), we think it is difficult to adapt any flux adjustment at the boundary, because imbalance between scalar and momentum fields can cause noises around the boundary. As for problem B), it seems that the resonance within the overlapped area is related to the issue. Baba et al. (2010) used the filter proposed by Shapiro (1971) to moderate problem around the boundary, and we found it really is effective through the one dimensional test for our scheme.

5. Future Plan

We plan to develop a three dimensional Yin-Yang grid model named “ASUCA –GLOBAL” on the K computer of the Japanese High Performance Computing Infrastructure (HPCI) project, and will examine its dynamical nature and computational efficiency. Fig. 10 presents preliminary results from execution at the current JMA’s computer.

We found the efficiency of the Shapiro’s filter in this study, however we have not used it yet, since Shapiro’s filter requires wider (more than eight grids) halo region and larger amount of MPI communication. We need to consider such issues in the near future.

6. Acknowledgement

This study is supported by the Program for Risk Information on Climate Change: SOUSEI.

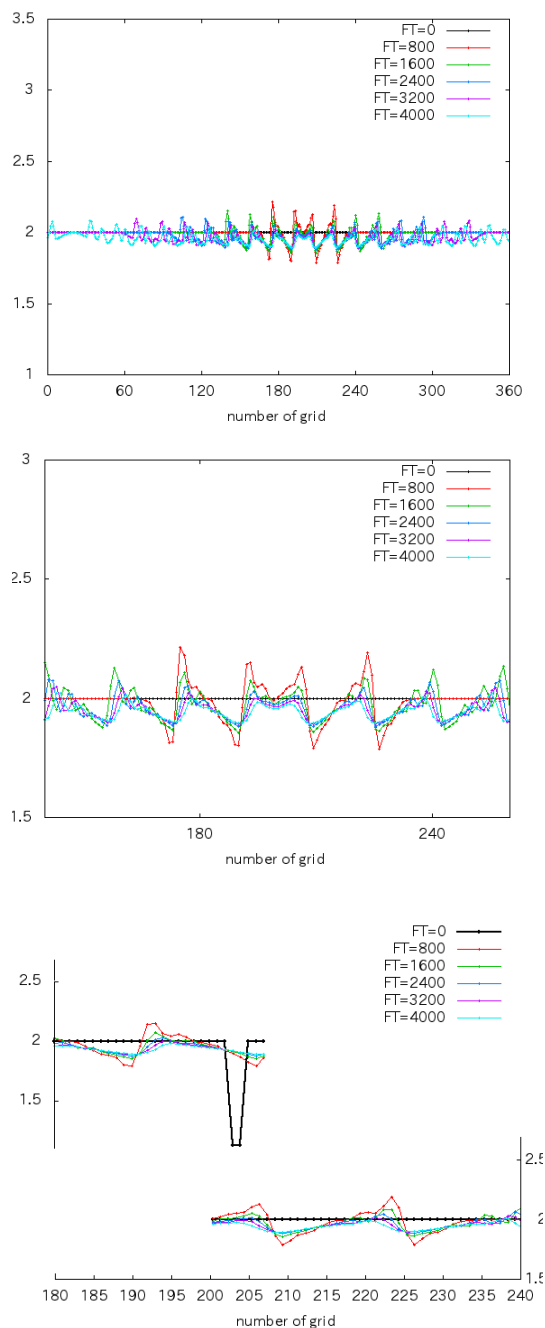


Fig. 9 The same figures as Fig. 8 with Shapiro (1971) and minor modifications in flux estimation and dynamics. The modifications include 4th order height estimation and 4th order gradient estimation by Levander (1988) in the gravity term, and the interface velocity calculation referring the 4 grids.

REFERENCES

Y. Baba, K. Takahashi, and T. Sugimura 2010: Dynamical Core of an Atmospheric General Circulation Model on a Yin-Yang Grid. *Mon. Wea. Rev.*, **138**, 3988-4005.

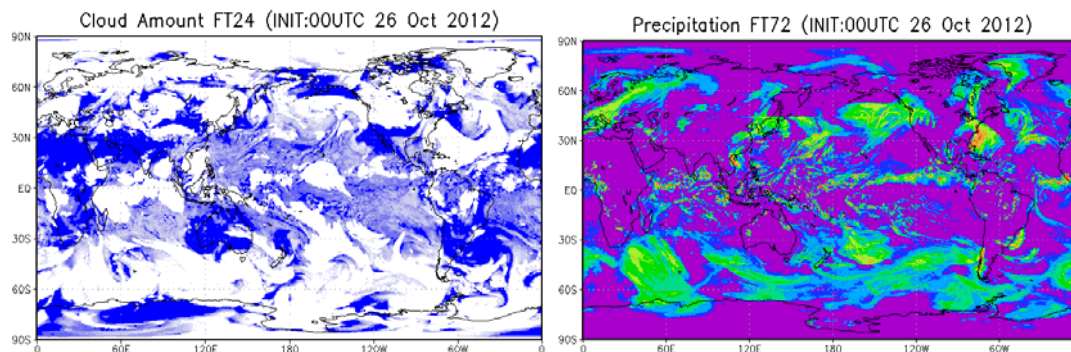


Fig.10 Forecast samples by “ASUCA-global”. A 24hour forecast of distribution of could amount starting at 00UTC 26 Oct. 2012 (left), and a 72 hour forecast of distribution of precipitation from the same initial time.

W. Hundsdorfer, B. Koren, M. Van Loon, and J. G. Verwer, 1995: A Positive Finite-Difference Advection Scheme. *J. Comp. Phys.* **117**, 35-46.

Ishida, J., C. Muroi, K. Kawano, and Y. Kitamura 2010: Development of a New Nonhydrostatic Model ASUCA at JMA. *CAS/JSC WGNE Research Activities in Atmospheric and Oceanic Modeling*.

A. Kageyama and T. Sato 2004: “Yin-Yang grid”: An overset grid in spherical geometry. *Geochem. Geophys. Geosys.* **VOL. 5**, Q09005, doi:10.1029/2004GC000734.

Koren, B, 1993: A robust upwind discretisation method for advection, diffusion and source terms. *Numerical Methods for Advection-Diffusion Problems, Vieweg, Braunschweig*, **117**.

Levander, A., 1988. Fourth-order finite-difference P-SV seismograms, *Geophysics*, **53**, 1425–1436.

X. Peng, F. Xiao, and K. Takahashi 2006: Conservative Constraint for a Quasi-Uniform Overset Grid on the Sphere. *Q.J.R. Met. Soc.*, **132**, 979-996.

Qaddouri, A., and V.Lee, 2011: The Canadian Global Environmental Multiscale model on the Yin-Yang grid system, *Quart. J. Roy. Meteor. Soc.*, **137**, 660, 1913-1926, DOI: 10.1002/qj.873.

R. Shapiro 1971: The Use of Linear Filtering as Parameterization of Atmospheric Diffusion. *J. Atmospheric Science*, **28**, 525 – 531.

T. Sugimura, K. Takahashi, and H. Sakagami 2006: Characteristics of Numerical Error on Overset Grid. *Nagare (in Japanese)*, **25**, 247-256.

L. J. Wicker and W. C. Skamarock 2002: Time-Splitting Methods for Elastic Models Using Forward Time Schemes. *Mon. Wea. Rev.* **130**, 2088 – 2097.

D. L. Williamson, J.B. Drake, J.J. Hack, R. Jakob, and P.N. Swarztrauber 1992: A Standard Test Set for Numerical Approximations to the Shallow Water Equations in Spherical Geometry. *J. Comp. Phys.* **102**, 211-224.